

Machine Learning to Predict Slot Usage in TSCH Wireless Sensor Networks

Stefano Scanzio*, Gabriele Formis*[†], Tullio Facchinetti[‡], Gianluca Cena*

*National Research Council of Italy (CNR-IEIT), Italy.

[†]Politecnico di Torino, Italy.

[‡]University of Pavia, Italy.

Emails: stefano.scanzio@cnr.it, gabriele.formis@polito.it, tullio.facchinetti@unipv.it,
gianluca.cena@cnr.it

Abstract—Wireless sensor networks (WSNs) are employed across a wide range of industrial applications where ultra-low power consumption is a critical prerequisite. At the same time, these systems must maintain a certain level of determinism to ensure reliable and predictable operation. In this view, time slotted channel hopping (TSCH) is a communication technology that meets both conditions, making it an attractive option for its usage in industrial WSNs.

This work proposes the use of machine learning to learn the traffic pattern generated in networks based on the TSCH protocol, in order to turn nodes into a deep sleep state when no transmission is planned and thus to improve the energy efficiency of the WSN. The ability of machine learning models to make good predictions at different network levels in a typical tree network topology was analyzed in depth, showing how their capabilities degrade while approaching the root of the tree. The application of these models on simulated data based on an accurate modeling of wireless sensor nodes indicates that the investigated algorithms can be suitably used to further and substantially reduce the power consumption of a TSCH network.

Index Terms—Time slotted channel hopping, ultra-low power, wireless sensor networks, machine learning, TSCH, WSN, ML.

I. INTRODUCTION

In the context of wireless networks, time division multiple access (TDMA) is a communication paradigm based on the slicing of time into slots of fixed duration. The TDMA concept is the main building block for enabling scheduling in such networks, providing the double advantages of increased determinism and reduced power consumption. The latter is obtained by turning the node into a deep sleep state when no transmission is scheduled for it in the considered time slot. Grounded on the concept of TDMA, the time slotted channel hopping (TSCH) operating mode described in the IEEE 802.15.4 standard [1] operates as TDMA in terms of time division into slots (time slotted), while adding the possibility of changing the transmission channel at every transmission, reducing the variability in performance due to the different quality of diverse channels (channel hopping) [2].

This work was partially supported by the European Union under the Italian National Recovery and Resilience Plan (NRRP) of NextGenerationEU, partnership on “Telecommunications of the Future” (PE00000001 - program “RESTART”).

At the same time, wireless sensor networks (WSNs) are gaining ground in the landscape of industrial networks, which are commonly characterized by a high level of heterogeneity in terms of communication technologies [3]. WSNs are used in all these industrial contexts, at the edge of the network [4], where sensing or actuation are not limited to strict timing constraints (hard deadlines), but on the contrary, low power consumption is the main target. This is common in applications such as environmental sensing for Heating, Ventilation and Air Conditioning (HVAC) systems, in product tracking, for predictive maintenance, in backup networks, or alarm systems [5]. In all these applications, the WSN follows a paradigm called *deploy and forget*, where battery-powered nodes are permanently placed in the environment under monitoring and must operate without external intervention for 10 years or more.

Among the several different protocols used for implementing WSNs (e.g., Zigbee, WirelessHART, ISA 100.11a, LoRaWAN, IO-Link Wireless, or Bluetooth Low Energy), in the context of industrial networks, TSCH has the dual advantage of providing a good level of determinism [6] and an energy consumption that is low enough to be suitable for the *deploy and forget* paradigm. Both properties derive from the time slotted characteristic of TSCH, which enables proper scheduling of network traffic [7]. In particular, when no transmission is scheduled for a given node in a specific time slot, the node can enter a deep sleep state, causing the node to consume a negligible amount of energy.

Like many WSN implementations, common TSCH networks are based on a tree routing topology, which is dynamically constructed by the routing protocol for low-power and lossy networks (RPL) [8]. In this case, values sensed and generated by leaf nodes are delivered through a multi-hop path to the sink node, i.e., the root of the tree.

On a single link of the tree, transmissions can occur only in given time intervals/slots as predefined by a schedule. Since typically these networks make use of a small subset of the scheduled slots, specific algorithms can be used to predict which slots are effectively used for transmissions. For unused slots, the node can enter a deep sleep state to significantly

reduce its power consumption.

This work investigates the application of machine learning (ML) approaches to the prediction of the patterns generated in a TSCH network.

Due to the tree topology of the network, moving from the leaves to the root node, the traffic flows generated by leaf nodes aggregate; this reduces the capability of predicting the used slots. One goal of this work is to examine how the performance of ML algorithms for the prediction of slot utilization degrades while approaching the root node. On the one hand, this performance degradation is a very important aspect that highlights one of the possible limitations of a data-driven approach to the addressed task. On the other hand, results demonstrate that the performance remains satisfactory. The analysis is done with energy savings in mind, for which the results reported in this paper show substantial reductions.

The paper is organized as follows. Section II analyzes the scientific literature about techniques to reduce power consumption in TSCH networks, while Section III reports the basic concepts behind TSCH and highlights some aspects related to power consumption. Section IV describes the mathematical framework for the prediction of slot utilization, the related results are commented in Section V, and Section VI finally concludes this work.

II. LITERATURE REVIEW

The research about reduction in energy consumption for WSN in general, and TSCH specifically, has been and is currently a very active area and direction of investigation.

Some researches involve all the nodes of the network as a whole, and they are based on global optimizations aimed at enhancing some performance indicators such as power consumption. In this context, a common strategy is to balance nodes' load to have a uniform discharge of nodes' batteries [9], or the tuning of specific network parameters to improve one or more key performance indicators such as latency, reliability, or power consumption [10]. It is important to notice that, typically, the optimization is subject to trade-offs; in other words, the improvement of one index leads to the worsening of the others.

Other techniques optimize specific protocols that are used in combination with TSCH to setup and manage the network. For instance, in [11], a more energy-efficient version of the RPL protocol, which is aimed at generating the network routing topology, is presented. In [12], the authors proposed an energy-efficient network formation mechanism.

In order to divide time into slots, nodes must operate in a synchronized manner [13]. The synchronization accuracy and efficiency of the protocol have a direct impact on power consumption. In [14], the guard time, which is used to make the protocol robust to not perfect synchronization, is adapted dynamically, while in [15] a dynamic modification of the sending period of enhanced beacons is proposed, which are directly used by the TSCH protocol for synchronization purposes.

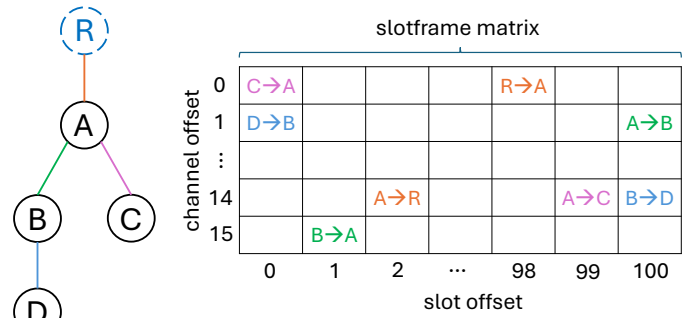


Fig. 1. Example of a TSCH slotframe matrix.

Techniques based on white and black listing permit the selection of the best communication channel or the removal of the worst channel in order to improve communication quality [16], [17]. Since this also reduces the number of retransmissions, it has a direct impact on energy consumption.

A very common way to reduce power consumption is by acting on scheduling properties. Following this approach, there are methods, such as the VAM-HSA algorithm [18], which reduce energy consumption by solving an energy-efficiency maximization problem, while [19] proposed a schedule procedure named PRCOS to maximize system lifetime. The method proposed in [20] extends the concept of scheduling to reduce energy consumption for battery-less devices.

Finally, proactive reduction of idle listening (PRIL) techniques take advantage of the periodicity of traffic to place nodes in deep sleep states when a scheduled slot is not used. In this context, PRIL-F [21], [22] was the first definition of the technique that acts only one hop away from the source of the traffic, while PRIL-M [23] overcomes this limitation. The PRIL techniques, even if quite different, are the most similar to the concepts described in this paper, but they do not rely on self-learning. Indeed, PRIL techniques make use of additional information added to packets for entering nodes into deep sleep states, whereas it is not the case for the ML technique presented in this work.

III. TSCH AND POWER CONSUMPTION

The TSCH protocol technology was first standardized in 2012, and it is currently included in the latest version of the IEEE 802.15.4 standard [1]. Unlike the deterministic and synchronous multi-channel extension (DSME) operating mode, in TSCH time is slotted similarly to TDMA. This feature increases latency predictability [10], [6], [24]. The TSCH operating mode defines the operation of a WSN network at the MAC layer. Protocol suites such as IPv6 over the TSCH mode of IEEE 802.15.4e (6TiSCH) [25], [26] embed and describe the interaction of a set of protocols in addition to TSCH (e.g., RPL to define routing) to provide the user with all the required components to setup a TSCH network. In addition to 6TiSCH,

where N_s is the source node, N_d is the destination node, P is the period, and R is the routing, i.e., an ordered sequence representing the nodes that need to be traversed to reach the destination. In the case of the example of Fig. 2, $R = (N_s, N_x, N_i, N_j, N_y, N_d)$, and involved links with corresponding levels are $N_s \xrightarrow{l=1} N_x$, $N_x \xrightarrow{l=2} N_i$, $N_i \xrightarrow{l=3} N_j$, $N_j \xrightarrow{l=4} N_y$, $N_y \xrightarrow{l=5} N_d$.

Let $x_k^{N_i \rightarrow N_j} = 1$ denote if a given link $N_i \rightarrow N_j$ is used (by flows crossing the link) for transmission at a discrete time k , while $x_k^{N_i \rightarrow N_j} = 0$ denotes if the link is not used. As already introduced, this latter condition is known as idle listening, a state in which the receiver node N_j activates its interface to receive a frame that will not arrive, resulting in a significant waste of energy. It is important to notice that, if the TSCH matrix contains only one scheduled link $N_i \rightarrow N_j$ between these two nodes, a value $x_k^{N_i \rightarrow N_j}$ is logged for every repetition of the slotframe matrix, which typical period is $T_{\text{matrix}} = 2.02$ s. If the same link $N_i \rightarrow N_j$ is present more than once in the TSCH matrix, it is counted according to the number of occurrences (i.e., each occurrence corresponds to the acquisition of a sample $x_k^{N_i \rightarrow N_j}$).

The ordered sequence of acquired samples $(x_1^{N_i \rightarrow N_j}, \dots, x_k^{N_i \rightarrow N_j}, \dots, x_N^{N_i \rightarrow N_j})$ is the dataset $\mathcal{D}^{N_i \rightarrow N_j}$ with cardinality N , which represents the slot usage for the link $N_i \rightarrow N_j$. To simplify the notation, when referring to a specific link, the notation $\mathcal{D} = (x_1, \dots, x_k, \dots, x_N)$ may be used directly without specifying the source and destination nodes, and $|\mathcal{D}|$ can be used in place of N .

For a given link $N_i \xrightarrow{l} N_j$, an ML model can be trained, given the usage statistics of the links. For this reason, the dataset \mathcal{D} was split into two disjoint datasets \mathcal{D}_{tr} and \mathcal{D}_{te} , with training and test data, respectively.

Let $x_k \in \mathcal{D}_{\text{tr}}$ be the current sample, the less recent n_p samples (i.e., $X_k = (x_k, x_{k-1}, \dots, x_{k-n_p+1})$) are used to train a model $f_M(\theta^*, \cdot)$ and to estimate its hyperparameters θ^* for the prediction of the next target x_{k+1} sample (i.e., if the slot associated to the link will be used for transmission or not). The trained ML model $f_M(\theta^*, X_k)$ is then used for the test dataset \mathcal{D}_{te} to predict x_{k+1} . As usual, the goal for the training procedure is to minimize the mean squared error (MSE) between the prediction and the target x_{k+1} :

$$\theta^* = \arg \min_{\theta} \sum_{k=n_p, \dots, |\mathcal{D}_{\text{tr}}|-1} \left(x_{k+1} - f_M(\theta, X_k) \right)^2, \quad (2)$$

where $|\mathcal{D}_{\text{tr}}|$ is the cardinality of the training dataset.

The main objective of this work is to study how the performance provided by ML models varies as the level changes in the case of periodic traffic patterns. For links related to leaf nodes, where $l = 1$, the occupation of specific slots by the traffic is quite predictable, while at higher levels, as approaching the root node, flows belonging to the underlying

nodes are increasingly mixed, and they become less and less predictable.

From an application perspective, a model $f_M^l(\theta^*, \cdot)$ could be trained for each link. In this article, we focus on how performance varies at different levels of the network topology. Since in the experimental campaign we selected only one link for each level, the information of the link on which the model is training is omitted in order to make the notation simpler.

As the objective of this paper was not to detect the best ML model but to analyze a generic model at different network levels, the very simple multilayer perceptron (MLP) model was selected. In addition, MLP can be implemented easily and efficiently, even in nodes with limited computational power. The MLP models exploited in this work consist of a two-layer neural network with $n_p = 890$ inputs, a hidden layer composed of 8 neurons with *ReLU* activation functions, and one output layer with a *sigmoid* activation function. The input vector X_k has a size of $n_p = 890$ corresponding to about 30 minutes, considering that the schedule of the TSCH matrix repeats over time every $T_{\text{matrix}} = 2.02$ s. The model was trained in 20 epochs using the *adam* optimizer and the MSE as loss function. The *batch size* was set equal to 32, and the learning rate was initialized to 0.01 and halved at each training epoch. The *Keras* module included in *TensorFlow* was used to manage both the training and the test phases of the model.

In addition, using the same test datasets \mathcal{D}_{te} used to assess the accuracy of the $f_M^l(\theta^*, \cdot)$ models, a statistical index that would give an indication of the difficulty in predicting the target at different levels has been computed.

In particular, to provide insight into the predictability of binary data, the normalized discrete autocorrelation was used:

$$\rho_k = \frac{R_k}{R_0}, \quad k \in \left[-\left\lfloor \frac{|\mathcal{D}_{\text{te}}|}{2} \right\rfloor, \dots, \left\lfloor \frac{|\mathcal{D}_{\text{te}}|}{2} \right\rfloor \right], \quad (3)$$

$$R_k = \sum_{n=1}^{|\mathcal{D}_{\text{te}}|} x_n \cdot x_{n+k}, \quad (4)$$

where R_k is the non-normalized discrete autocorrelation.

High values of ρ_k indicate that the vector corresponding to \mathcal{D}_{te} and the same vector translated by a quantity k are strongly related, and consequently, their content is more predictable. On the contrary, low autocorrelation suggests a weak or no linear dependence with previous values, and consequently, data that is difficult to predict. By definition, $\rho_0 = 1$ and $\rho_k = \rho_{-k}$.

In particular, the evolution of the maximum value of the autocorrelation ρ_{max}^l of links at different network levels l is analyzed in the next result section:

$$\rho_{\text{max}}^l = \max_{k \neq 0} \rho_k. \quad (5)$$

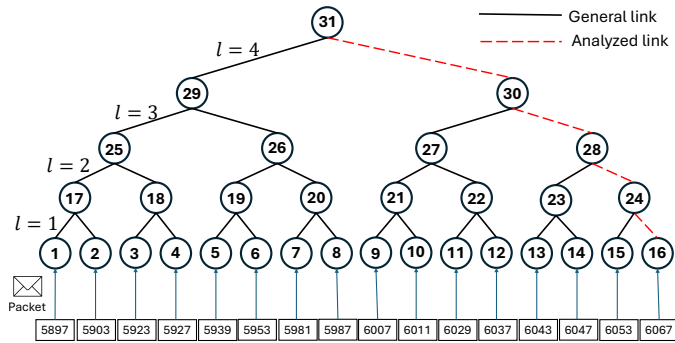


Fig. 3. Topology of the network considered in the experimental analysis.

TABLE I
MAIN SIMULATION PARAMETERS.

Quantity	Description	Typical value
N_{slot}	Number of slots in a TSCH matrix	101
T_{slot}	Duration of a slot	20 ms
T_{matrix}	Duration of the TSCH matrix	2.02 s
N_{try}	Maximum number of tries	16
ϵ_{frame}	Data frame success probability	0.874
ϵ_{ACK}	ACK frame success probability	0.92
T_{sim}	Duration of the simulation	20 years
E_{tx}	Energy to transmit data and receive ACK	266 μJ
E_{rx}	Energy to receive data and transmit ACK	284 μJ
E_{listen}	Energy for idle listening (wasted)	138 μJ

V. RESULTS

The experimental campaign was carried out on the network reported in Fig. 3, which is a 4-layer network composed of 31 nodes. Packet flows are generated by leaf nodes, numbered from N_1 to N_{16} , and the generation periods are reported in the rectangles below the nodes. The path for which results are reported and discussed is highlighted with a dashed red line. However, experimental results for the other paths are similar and are not reported here for space reasons.

A. Dataset acquisition

The dataset was acquired by means of the TSCHmodeler discrete event simulator, which was already used in [28]. An initial experimental campaign was conducted (details not included here for brevity) that demonstrates how the results from the simulator are very similar to those obtained from actual TSCH implementation based on OpenMote B devices running OpenWSN protocol stack (6TiSCH).

The main simulation parameters are summarized in Table I. Concerning the number of slots in the TSCH matrix, the duration of the single slot, the duration of the TSCH matrix, and the maximum number of allowed transmission attempts,

TABLE II
CONFIGURATION OF THE TSCH MATRIX USED IN THE EXPERIMENTAL CAMPAIGN (IN **BOLD**, ANALYZED LINKS).

Slot Offset	Source Node	Dest. Node	Slot Offset	Source Node	Dest. Node
9	11	22	45	22	27
13	1	17	46	24	28
15	18	25	50	16	24
19	26	29	57	13	23
20	27	30	59	15	24
21	30	31	66	25	29
28	20	26	67	6	19
31	7	20	70	28	30
32	9	21	78	2	17
33	19	26	82	23	28
34	8	20	83	5	19
35	29	31	84	12	22
37	10	21	85	17	25
38	14	23	89	3	18
40	21	27	96	4	18

we set the default values used by OpenWSN for OpenMode B nodes, i.e., $N_{\text{slot}} = 101$, $T_{\text{slot}} = 20$ ms, $T_{\text{matrix}} = 2.02$ s, $N_{\text{try}} = 16$.

The value of the data and ACK frames success probability (i.e., $\epsilon_{\text{frame}} = 0.874$ and $\epsilon_{\text{ack}} = 0.92$, respectively) were obtained from [22], and they are based on data derived from a real testbed based on the OpenWSN implementation of the TSCH protocol. The length of the simulation was set equal to 20 years. The first 12 611 881 samples were used for \mathcal{D}_{tr} , while the latter 3 000 000 samples were used for \mathcal{D}_{te} (i.e., $|\mathcal{D}_{\text{tr}}| = 12\,611\,881$ and $|\mathcal{D}_{\text{te}}| = 3\,000\,000$ samples).

Regarding power consumption, the measurements described in [10] for OpenMote B devices installed with OpenWSN were used as reference. It is interesting to notice that the energy to transmit a data frame of maximum dimension $E_{\text{tx}} = 266 \mu\text{J}$ (and receive the related ACK frame) or to receive a data frame of the same maximum dimension $E_{\text{rx}} = 284 \mu\text{J}$ (and to send the related ACK frame) are almost the same. Instead, the energy wasted due to idle listening $E_{\text{listen}} = 138 \mu\text{J}$ is almost half E_{tx} and E_{rx} . This means that the waste of energy due to idle listening is quite high, considering the fact that for this type of network, most of the scheduled slots are typically unused. Other devices are characterized by different consumption. For instance, OpenMoteSTM devices have the following values in terms of power consumption, $E_{\text{tx}} = 485.7 \mu\text{J}$, $E_{\text{rx}} = 651.0 \mu\text{J}$, $E_{\text{listen}} = 303.3 \mu\text{J}$ [27], but in any case, the waste of energy related to idle listening remains significant.

The configuration of the TSCH matrix used in the experimental campaign was reported in Table II, in which the slot

offset used for every link of the network in Fig. 3 was selected randomly. The channel offset was not reported since we set ϵ_{frame} and ϵ_{ACK} equal for all channels.

In Table II and in Fig. 3, the links $N_{16} \xrightarrow{l=1} N_{24}$, $N_{24} \xrightarrow{l=2} N_{28}$, $N_{28} \xrightarrow{l=3} N_{30}$, $N_{30} \xrightarrow{l=4} N_{31}$ are highlighted since they are those for which different performance metrics have been reported and analyzed.

In the experimental setup proposed in this work, traffic flows are generated by leaf nodes, one for each leaf. Traffic is periodic, as is typical for this kind of network. The generation period for each flow was intentionally chosen to be different from the other flows. This decision was made to reflect the fact that in typical real networks, packet generation by applications is not synchronized with the network slots. In particular, the generation period measured in terms of time slot was reported in the lower part of Fig. 3.

B. Autocorrelation and Prediction Quality

The datasets obtained for the four links at different levels were used to train the corresponding models $f_M^{l=1}(\cdot)$, $f_M^{l=2}(\cdot)$, $f_M^{l=3}(\cdot)$, and $f_M^{l=4}(\cdot)$.

The results evaluated on the test datasets \mathcal{D}_{te} for the four links are reported in Tables III. The upper Table III reports the values of the confusion matrices for different levels, namely: *true positive* (TP, i.e., slots actually used that are predicted as used), *false negative* (FN, i.e., slots actually used that are predicted as not used), *false positive* (FP, i.e., slots actually not used that are predicted as used), and *true negative* (TN, i.e., slots actually not used that are predicted as not used).

Regarding the lower Table III, the first column represents the maximum normalized discrete autocorrelation ρ_{max}^l . As expected, it is inversely proportional to the level l , and it reflects the growing complexity of the prediction task as levels increase. As previously mentioned, this occurs since traffic flows generated by nodes at the leaf level mix together in an unpredictable way.

TABLE III
CONFUSION MATRIX AND PERFORMANCE METRICS AT DIFFERENT LEVELS

Quantity	$l = 1$	$l = 2$	$l = 3$	$l = 4$
True Positive (TP)	48444	92363	167481	312544
False Negative (FN)	13631	32017	81728	186919
False Positive (FP)	0	17034	52643	163289
True Negative (TN)	2937035	2857696	2697258	2336358

Link/Level	ρ_{max}^l	Acc.	Prec.	Rec.	F1 score	AUC
$N_{16} \xrightarrow{l=1} N_{24}$	0.986	0.995	1.000	0.780	0.877	0.998
$N_{24} \xrightarrow{l=2} N_{28}$	0.943	0.984	0.844	0.743	0.790	0.992
$N_{28} \xrightarrow{l=3} N_{30}$	0.855	0.955	0.761	0.672	0.714	0.976
$N_{30} \xrightarrow{l=4} N_{31}$	0.678	0.883	0.657	0.626	0.641	0.926

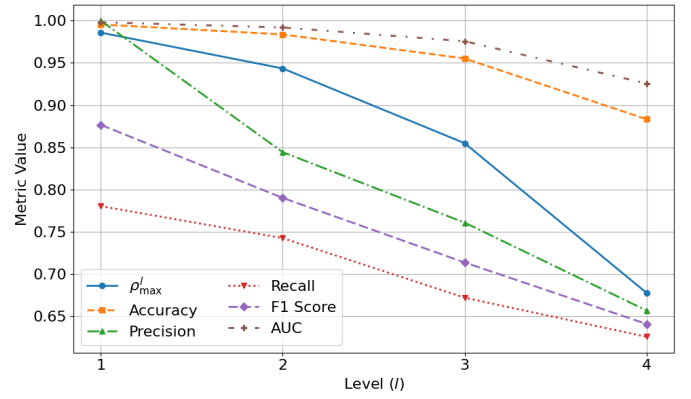


Fig. 4. The evolution of key quality indicators as levels change.

The other five columns represent, in order, the *accuracy* (i.e., how often the prediction of $f_M(\theta^*, \cdot)$ is correct), the *precision* (i.e., the percentage of predicted used slots that are actually used), the *recall* or *sensitivity* (i.e., how many actual used slots are correctly predicted), the *F1 scores* (i.e., a harmonic mean of precision and recall), and the *AUC* that is an index ranging from 1.0 (i.e., perfect prediction) to 0.5 (i.e., random prediction). All these performance indicators can be computed directly from the confusion matrices reported in the upper table.

As highlighted by the table, all indices, in a different way, reflect a substantial decrease in performance as the level increases.

The plot of Fig. 4 reports the evolution of the quality indices reported in Table III as the level increases. As can be noticed, the most affected indices are precision and F1 score, since they have a sharper decreasing slope.

Regardless of the level, all the models exhibited a reasonably good prediction quality. In particular, the accuracy index shows that slots predicted as used have a probability of 88.3% (in the most complex condition regarding $l = 4$) of being effectively used by nodes. Unfortunately, as highlighted by the recall index, there are some slots that are predicted as not used for transmission, for which a transmission occurs. In this case, the transmission is delayed to the next available slot associated with the link, which is predicted as usable by the model. This increases the transmission latency, which may be acceptable for many application contexts of this type of network, where, in many cases, the main goal is to optimize power consumption.

This investigation is aimed at verifying the ability of ML models to predict slot usage at different levels of a TSCH/TDMA network. For the integration of the mechanism in a real TSCH network, some small modifications to the protocol are needed. In particular, since the ML model is intentionally not aware of the number of messages in the queue of the sender node, it might predict that a slot is not

TABLE IV
ENERGY CONSUMPTION OF A SPECIFIC LINK VS. LEVEL

Quantity	$l = 1$	$l = 2$	$l = 3$	$l = 4$
$P_{tx} (\mu W)$	2.73	5.46	10.94	21.92
$P_{rx} (\mu W)$	2.91	5.83	11.68	23.41
$P_{listen} (\mu W)$	0.00	0.39	1.20	3.72
$P_{listen}^{-ML} (\mu W)$	66.88	65.46	62.62	56.92

usable even if it has some frames ready for transmission in its transmission queue.

To avoid this problem, if the transmission queue contains, in addition to the packet that is currently transmitted, another packet addressed to the same destination node (i.e., related to the same link), the transmitter has to add to the current transmitted packet an indication that the queue is not empty. In this way, even if the ML model predicts that the slot will not be used, the receiver will remain active in reception when the same link is scheduled for the next time. To this extent, the TSCH protocol provides specific *information elements*, which are user-defined information that can be included in the MAC header. In the context of this work, the information element is added to notify the receiver if the queue is not empty.

In the case of loss of a data packet, it is retransmitted in the next slot, which is marked as usable by the ML algorithm. If the queue starts to grow, meaning that more frames have arrived in the meantime after the packet to be retransmitted, the system adapts to prevent the queue from increasing indefinitely. As described, this operation is performed by including an information element in the transmitted packet that disables the ML algorithm responsible for predicting slot usage.

C. Energy consumption

The main target of the proposed analysis is the use of ML algorithms for traffic prediction aimed at reducing power consumption.

Even if the exact computation of the energy saved can be performed only by means of a complete implementation of the proposed algorithm, including the optimizations based on information elements described in the previous subsection, some considerations can be derived directly from the results obtained in this context.

Specifically, the value reported in Table IV, are obtained from the confusion matrices reported on Table III. The number of transmissions and related receptions can be approximated as TP+FN, where FN refers to the slots that should be exploited for transmission but the ML algorithm has chosen not to utilize. It is not an error to count them in the computation of energy consumption, since these transmissions are performed in any case, but using different slots. For the exchange of messages, referred to a specific link, the power consumed by the node is:

$$P_{tx} = \frac{(TP + FN) \cdot E_{tx}}{|\mathcal{D}_{te}| \cdot T_{matrix}}, \quad (6)$$

$$P_{rx} = \frac{(TP + FN) \cdot E_{rx}}{|\mathcal{D}_{te}| \cdot T_{matrix}}, \quad (7)$$

where the denominator $|\mathcal{D}_{te}| \cdot T_{matrix}$ represents the duration in seconds of the test dataset \mathcal{D}_{te} .

The mechanism proposed in this work acts by preventing idle listening by not turning on the node in reception if the ML algorithm does not predict the usage of the slot. Consequently, TN represents those slots for which the node is set in a sleep state since they are not used for transmission, while FP represents those slots that suffer from idle listening because their usage is not properly predicted by the ML algorithm. The additional power wasted for idle listening is:

$$P_{listen} = \frac{n_{listen} \cdot E_{listen}}{|\mathcal{D}_{te}| \cdot T_{matrix}}, \quad (8)$$

where $n_{listen} = FP$. If in (8) we substitute $n_{listen} = FP + TN$, we obtain P_{listen}^{-ML} , which represents the energy wasted for idle listening for a typical TSCH implementation without the use of ML to predict slots utilization.

As highlighted by the results reported in Table IV, the component of idle listening, which is predominant in the communication, is nevertheless completely eliminated in practice. In the worst operating condition, corresponding to $l = 4$, P_{listen} is reduced to $3.72 \mu W$, which has to be compared with the unmodified TSCH implementation where $P_{listen}^{-ML} = 56.92 \mu W$. As expected, for links closer to the root node, the capability of the ML model to predict slot usage decreases, and the energy waste slightly increases.

VI. CONCLUSIONS

This paper investigated the performance of machine learning algorithms to capture the traffic patterns generated by the TSCH communication protocol for WSNs, at different distances from the source nodes in multi-hop networks. Its final goal is the use of the inferred information to reduce the energy usage of the sensor nodes by turning the nodes in deep sleep mode when they are not actively involved in the communication.

Experimental results show the effectiveness of the proposed approach while highlighting the negative impact of the network topology in terms of hops on the performance of the algorithm. These results open several interesting future perspectives, including the definition of all the details to integrate the mechanism in the TSCH protocol, and the experimentation of different network topologies, machine learning algorithms, and traffic patterns.

The main limitation, and at the same time source of inspiration for future work, is that this paper does not account for the extra energy required for machine learning algorithms to run on the node. Additionally, only cyclic generation patterns were analyzed, which are nevertheless the most common in the application context of this kind of WSNs.

REFERENCES

- [1] "IEEE Standard for Low-Rate Wireless Networks," *IEEE Std 802.15.4-2020 (Revision of IEEE Std 802.15.4-2015)*, pp. 1–800, 2020.
- [2] G. Cena, S. Scanzio, M. G. Vakili, C. G. Demartini, and A. Valenzano, "Assessing the Effectiveness of Channel Hopping in IEEE 802.15.4 TSCH Networks," *IEEE Open Journal of the Industrial Electronics Society*, vol. 4, pp. 214–229, 2023.
- [3] S. Scanzio, L. Wisniewski, and P. Gaj, "Heterogeneous and dependable networks in industry – A survey," *Computers in Industry*, vol. 125, p. 103388, 2021.
- [4] D. Rekha and L. Pavithra, "TSCH in Edge IoT: A Comprehensive Survey of Research Challenges," *Transactions on Emerging Telecommunications Technologies*, vol. 36, no. 3, p. e70088, 2025.
- [5] M. Majid, S. Habib, A. R. Javed, M. Rizwan, G. Srivastava, T. R. Gadekallu, and J. C.-W. Lin, "Applications of wireless sensor networks and internet of things frameworks in the industry revolution 4.0: A systematic literature review," *Sensors*, vol. 22, no. 6, p. 2087, 2022.
- [6] G. Cena, C. G. Demartini, M. Ghazi Vakili, S. Scanzio, A. Valenzano, and C. Zunino, "Evaluating and Modeling IEEE 802.15.4 TSCH Resilience against Wi-Fi Interference in New-Generation Highly-Dependable Wireless Sensor Networks," *Ad Hoc Networks*, vol. 106, p. 102199, 2020.
- [7] M. Balbi, L. Doherty, and T. Watteyne, "A comprehensive survey on channel hopping and scheduling enhancements for TSCH networks," *Journal of Network and Computer Applications*, vol. 238, p. 104164, 2025.
- [8] M. Zirak, Y. Sedaghat, and M. H. Y. Moghaddam, "RPL-TSCH cross-layer design for improve quality of service in LLNs of IIoT," *Ad Hoc Networks*, vol. 174, p. 103843, 2025.
- [9] S. Afshari, M. Nassiri, and R. Mohammadi, "SA-RPL: a scheduling-aware forwarding mechanism in RPL/TSCH-operated networks," *International Journal of Ad Hoc and Ubiquitous Computing*, vol. 34, no. 1, pp. 35–44, 2020.
- [10] S. Scanzio, M. G. Vakili, G. Cena, C. G. Demartini, B. Montrucchio, A. Valenzano, and C. Zunino, "Wireless Sensor Networks and TSCH: A Compromise Between Reliability, Power Consumption, and Latency," *IEEE Access*, vol. 8, pp. 167 042–167 058, 2020.
- [11] H. Farag, P. Österberg, M. Gidlund, and S. Han, "RMA-RP: A Reliable Mobility-Aware Routing Protocol for Industrial IoT Networks," in *IEEE Global Conference on Internet of Things (GCIoT 2019)*, 2019, pp. 1–6.
- [12] M. Mohamadi, B. Djamaa, and M. R. Senouci, "RAST: Rapid and energy-efficient network formation in TSCH-based Industrial Internet of Things," *Computer Communications*, vol. 183, pp. 1–18, 2022.
- [13] M. Mongelli and S. Scanzio, "A neural approach to synchronization in wireless networks with heterogeneous sources of noise," *Ad Hoc Networks*, vol. 49, pp. 1–16, 2016.
- [14] A. Mavromatis, G. Z. Papadopoulos, A. Elsts, N. Montavont, R. Piechocki, T. Tryfonas, G. Oikonomou, and X. Fafoutis, "Adaptive Guard Time for Energy-Efficient IEEE 802.15.4 TSCH Networks," in *Wired/Wireless Internet Communications*, M. Di Felice, E. Natalizio, R. Bruno, and A. Kassler, Eds. Cham: Springer International Publishing, 2019, pp. 15–26.
- [15] J. Vera-Pérez, D. Todolí-Ferrandis, J. Silvestre-Blanes, and V. Sempere-Payá, "Bell-X, An Opportunistic Time Synchronization Mechanism for Scheduled Wireless Sensor Networks," *Sensors*, vol. 19, no. 19, 2019.
- [16] G. Cena, S. Scanzio, and A. Valenzano, "Ultra-Low Power Wireless Sensor Networks Based on Time Slotted Channel Hopping with Probabilistic Blacklisting," *Electronics*, vol. 11, no. 3, p. 304, Jan 2022.
- [17] W. Jerbi, O. Cheickhrouhou, A. Guermazi, and H. Trabelsi, "MSU-TSCH: A Mobile scheduling updated algorithm for TSCH in the internet of things," *IEEE Transactions on Industrial Informatics*, pp. 1–8, 2022.
- [18] M. Ojo, S. Giordano, G. Portaluri, D. Adami, and M. Pagano, "An energy efficient centralized scheduling scheme in TSCH networks," in *IEEE International Conference on Communications Workshops (ICC)*, 2017, pp. 570–575.
- [19] T. Matsui and H. Nishi, "Time slotted channel hopping scheduling based on the energy consumption of wireless sensor networks," in *IEEE 15th International Workshop on Advanced Motion Control (AMC 2018)*, 2018, pp. 605–610.
- [20] D. van Leemput, J. Famaey, J. Hoebeke, and E. de Poorter, "Energy-Aware Adaptive Scheduling for Battery-Less 6TiSCH Routers in Industrial Wireless Sensor Networks," *IEEE Access*, vol. 12, pp. 180 034–180 047, 2024.
- [21] S. Scanzio, G. Cena, A. Valenzano, and C. Zunino, "Energy Saving in TSCH Networks by Means of Proactive Reduction of Idle Listening," in *Ad-Hoc, Mobile, and Wireless Networks*, L. A. Grieco, G. Boggia, G. Piro, Y. Jararweh, and C. Campolo, Eds. Cham: Springer International Publishing, 2020, pp. 131–144.
- [22] S. Scanzio, G. Cena, and A. Valenzano, "Enhanced Energy-Saving Mechanisms in TSCH Networks for the IIoT: The PRIL Approach," *IEEE Transactions on Industrial Informatics*, pp. 1–11, 2022.
- [23] S. Scanzio, F. Quarta, G. Paolini, G. Formis, and G. Cena, "Ultralow Power and Green TSCH-Based WSNs With Proactive Reduction of Idle Listening," *IEEE Internet of Things Journal*, vol. 11, no. 17, pp. 29 076–29 088, 2024.
- [24] Y. Shudrenko and A. Timm-Giel, "Modeling end-to-end delays in TSCH wireless sensor networks using queuing theory and combinatorics," *Computing*, vol. 106, no. 9, pp. 2923–2947, Sep 2024.
- [25] P. Thubert, "An Architecture for IPv6 over the Time-Slotted Channel Hopping Mode of IEEE 802.15.4 (6TiSCH)," *IETF RFC 9030*, pp. 1–57, May 2021.
- [26] X. Vilajosana, T. Watteyne, T. Chang, M. Vučinić, S. Duquennoy, and P. Thubert, "IETF 6TiSCH: A Tutorial," *IEEE Communications Surveys Tutorials*, vol. 22, no. 1, pp. 595–615, 2020.
- [27] X. Vilajosana, Q. Wang, F. Chraim, T. Watteyne, T. Chang, and K. S. J. Pister, "A Realistic Energy Consumption Model for TSCH Networks," *IEEE Sensors Journal*, vol. 14, no. 2, pp. 482–489, Feb 2014.
- [28] S. Scanzio, G. Formis, T. Facchinetti, G. Paolini, and G. Cena, "Wireless Sensor Networks Based on TSCH/TDMA with Power Consumption and Latency Constraints," in *2024 IEEE 29th International Conference on Emerging Technologies and Factory Automation (ETFA)*, 2024, pp. 1–4.